Zachary E. Loparo
Center for Advanced Turbomachinery and Energy Research (CATER),
Mechanical and Aerospace Engineering,
University of Central Florida,
Orlando, FL 32816

Andrey V. Muraviev
Department of Physics,
CREOL, The College of Optics and Photonics,
Nano Science Technology Center (NSTC),
University of Central Florida,
Orlando, FL 32816;
Truventic LLC,
Orlando, FL 32805

Pedro Figueiredo
Department of Physics,
Nano Science Technology Center (NSTC),
University of Central Florida,
Orlando, FL 32816

Arkadiy Lyakh
Department of Physics,
CREOL, The College of Optics and Photonics,
Nano Science Technology Center (NSTC),
University of Central Florida,
Orlando, FL 32816

Robert E. Peale
Department of Physics,
University of Central Florida,
Orlando, FL 32816;
Truventic LLC,
Orlando, FL 32805

Kareem Ahmed
Center for Advanced Turbomachinery and Energy Research (CATER),
Mechanical and Aerospace Engineering,
University of Central Florida,
Orlando, FL 32816

Subith S. Vasu
Center for Advanced Turbomachinery and Energy Research (CATER),
Mechanical and Aerospace Engineering,
University of Central Florida,
Orlando, FL 32816

Shock Tube Demonstration of Acousto-Optically Modulated Quantum Cascade Laser as a Broadband, Time-Resolved Combustion Diagnostic

We provide the first demonstration of an acousto-optically modulated quantum cascade laser (AOM QCL) system as a diagnostic for combustion by measuring nitric oxide (NO), a highly regulated emission produced in gas turbines. The system provides time-resolved broadband spectral measurements of the present gas species via a single line of sight measurement, offering advantages over widely used narrowband absorption spectroscopy (e.g., the potential for simultaneous multispecies measurements using a single laser) and considerably faster (>15 kHz rates and potentially up to MHz) than sampling techniques, which employ fourier transform infrared (FTIR) or GC/MS. The developed AOM QCL system yields fast tunable output covering a spectral range of 1725–1930 cm^{-1} with a linewidth of 10–15 cm^{-1}. For the demonstration experiment, the AOM QCL system has been used to obtain time-resolved spectral measurements of NO formation during the shock heating of mixture of a 10% nitrous oxide (N_2O) in a balance of argon over a temperature range of 1245–2517 K and a pressure range of 3.6–5.8 atm. Results were in good agreement with chemical kinetic simulations. The system shows revolutionary promise for making simultaneous time-resolved measurements of multiple species concentrations and temperature with a single line of sight measurement. [DOI: 10.1115/1.4040381]

Introduction and Background

Combustion technologies have been constantly evolving toward leaner, high-pressure, high-efficiency, and advanced oxy-fuel cycles [1–4]. Alternative fuels are increasingly considered for use with traditional and newer combustion engines [5–8]. It is of great interest to measure and model concentrations of emission species, such as NO_x, CO, and unburned hydrocarbons from gas turbines and powerplants [9,10]. In situ, time-resolved measurements of species during their formation and evolution would provide better understanding of the combustion process and thereby aid the development of high-efficiency and low-emission advanced gas turbines [11]. Existing and widely used methods for measuring in situ species concentrations in combustion systems using midinfrared (MIR) laser absorption spectroscopy have been spectrally narrow. For instance, absorption spectroscopy at a single wavelength coincident with the absorption of a species of interest is well established [12–14]. This technique generally requires a dedicated laser and detector for each species to be measured. Because absorption spectra of gaseous species change with temperature and pressure, a fixed wavelength may not be optimal over a wide range of temperatures and pressures.

Better chemical specificity is achieved by using differential absorption with two fixed wavelengths [15], which enables species identification and quantification even in the presence of interfering absorbers. This may be done with two lasers or more economically with one conventionally tunable laser. The latter case requires repeatable combustion events, which are

Contributed by the Advanced Energy Systems Division of ASME for publication in the Journal of Energy Resources Technology. Manuscript received May 10, 2018; final manuscript received May 13, 2018; published online June 12, 2018. Editor: Hameed Metghalchi.

difficult to achieve, introducing additional uncertainty and inconsistencies.

Fast wavelength modulation spectroscopy using infrared quantum cascade lasers (QCL) gives few-wavenumber periodic scanning by modulating the laser drive current [16], allowing real-time measurement of absorption fine structure to determine concentration and temperature. However, the tuning range is generally quite narrow and thus is generally inapplicable to measuring multiple species simultaneously.

In this work, we demonstrate the development and application of a fast-tuning broadband QCL that can identify multiple chemical species during a turbulent combustion reaction in a shock tube at time scales comparable to the characteristic times for variation of concentrations. The diagnostic scheme measures time-resolved absorption spectra over 1725–1930 cm^{-1}, a portion of the MIR spectral range which contains absorption features of highly regulated emission species including formaldehyde and nitric oxide (NO). In the experiments performed in this study, NO is identified as a reaction product by its characteristic spectral line shape as its concentration was measured at temperatures up to 2517 K and pressures up to 5.8 atm over the complete several millisecond duration of the shock tube experiments of the decomposition of shock heated nitrous oxide (N_2O) with a time resolution of 65 μs. This preliminary validation demonstrates the system's sensitivity to temperature and capability to obtain the concentration time-history of a species of interest.

Experiment

Acousto-Optically Modulated Quantum Cascade Laser System. The QCL was developed inhouse and was operated in an external cavity configuration with an intracavity AOM as described in Refs. [17–19]. A schematic of the setup is shown in Fig. 1.

The laser cavity is formed by the uncoated front (output) facet of the QCL chip and the high reflectivity back mirror after the AOM. The RF generator produces a traveling acoustic wave in the germanium AOM, creating a phase grating which Bragg-reflects the beam traveling through the crystal. The wavelength deflected toward the cavity back mirror is selected by changing the AOM modulation frequency, thus spectrally tuning the laser output. The QCL temperature is thermoelectrically regulated.

The selected wavelength can be changed in as little as ~1 μs [19], which is much faster than possible by usual mechanically tuned Littrow gratings. This makes the system attractive as a combustion diagnostic to obtain temporally resolved spectral measurements of combustion processes, where chemical concentrations change on a time scale of ~20 μs. The mid-IR QCL output range coincides with the molecular "fingerprint" region. The 5.5 μm center frequency of the QCL used here, and its ~200 cm^{-1} gain bandwidth, coincide with absorption features of NO and other combustion intermediates of interest including formaldehyde.

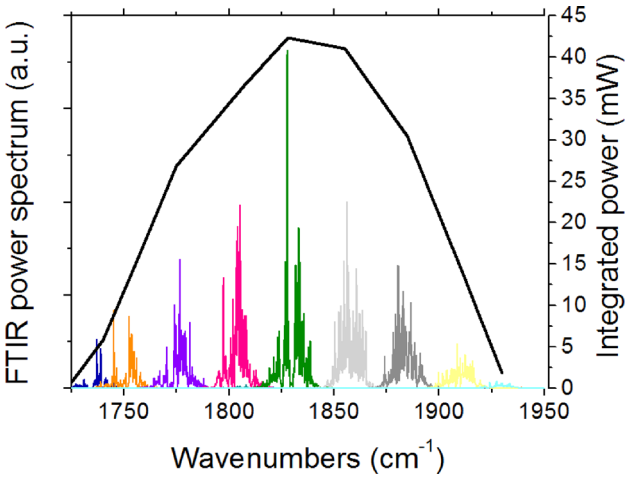

Fig. 2: Output intensity and measured spectra of different laser output lines for the AOM QCL system. The thick black line gives integrated intensity for each (colored) emission spectrum obtained by a different AOM modulation frequency.

Figure 2 presents fourier transform infrared (FTIR) spectra of the system for different RF frequencies applied to the AOM. The solid curve gives the spectrally integrated power for the individual spectra. The system's 205 cm^{-1} spectral bandwidth spans from 1725 to 1930 cm^{-1} (5.2–5.8 μm wavelength) with a maximum output power of 40 mW. The width of the emission band for the individual spectra ranges from 8 to 20 cm^{-1}.

Shock Tube Facility and Diagnostic Configuration. Shock tubes are ideal laboratory devices for producing controlled high-temperature and pressure conditions that exist inside gas turbines. Measurements were performed in a stainless-steel, heated, double-diaphragm shock tube with an inner diameter of 14 cm, located at the University of Central Florida, which has been described in our prior work [3,12–14,20–22]. The driver and driven sections of the shock tube are separated by a polycarbonate diaphragm 0.381 mm thick which suddenly ruptures to create a normal shock wave which shock heats the test mixture. Transmission spectra were collected 2 cm from the end wall of the shock tube, where access ports are arranged around the circumference of the tube. One port contained a Kistler 603B1 piezoelectric transducer to measure pressure in the reflected shock region. A pair of wedged ZnSe windows (3 mm thick × 12.7 mm diameter) were mounted in two opposing access ports for infrared transmission. Five piezoelectric pressure transducers (PCB113B26, 500 kHz frequency response) were placed along the last 1.4 m of the driven section to measure incident shock velocity, which was then

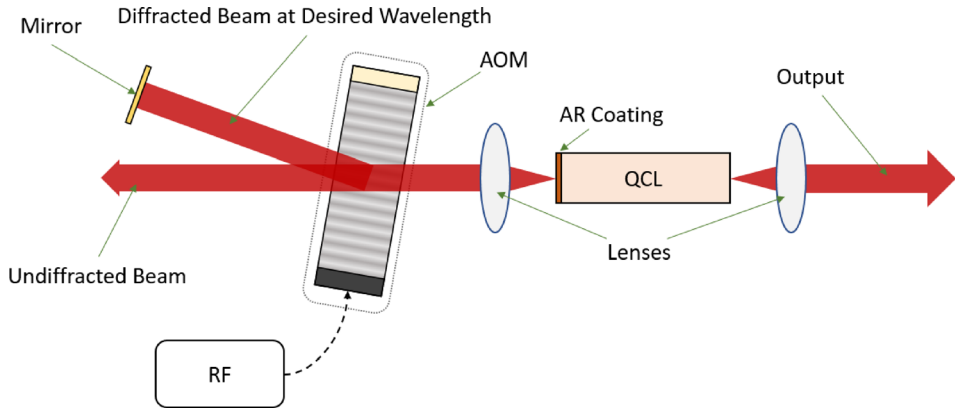

Fig. 1 Schematic of AOM QCL system (Adapted from [17–19])

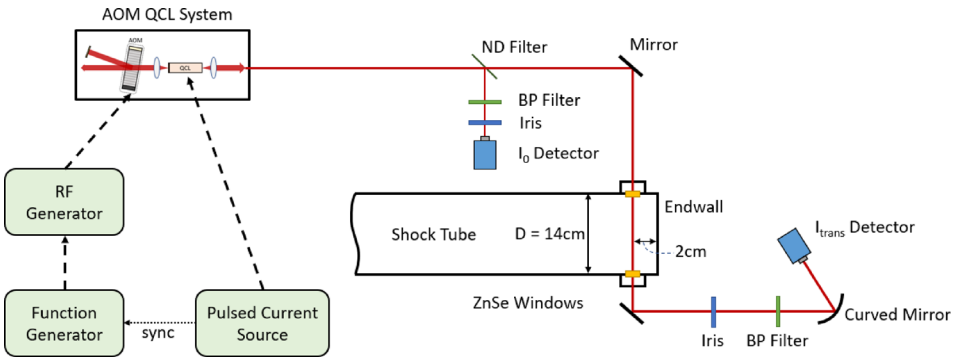

Fig. 3 Schematic of the optical setup of the AOM QCL system and the shock tube test section. (ND = neutral density, BP = bandpass).

linearly extrapolated to the endwall. The temperature and pressure (T_5 and P_5) in the reflected shock region are calculated using the initial temperature and pressure of the driven section (T_1 and P_1) and extrapolated shock velocity using one-dimensional shock relations, assuming chemically frozen, vibrationally equilibrated gases. Incident shock attenuation was always less than 1%, and uncertainty in temperature and pressure in the reflected shock region are estimated to be less than ±2% [12–14].

The experimental setup for spectral diagnostics of combustion processes using the fast-tuning AOM QCL system with a shock tube facility is presented in Fig. 3. A neutral density filter of optical density 1.0 split the QCL output into reference and signal beams. The intensity of the reference beam (I_0) was recorded by a thermoelectrically cooled photovoltaic detector (Vigo PVI-3TE-10.6, DC-1 MHz frequency bandwidth). The signal beam was passed through the shock tube and incident on a second identical photovoltaic detector to record transmitted signal (I_{trans}). A bandpass filter with a transmission range of 5–6 μm at the signal detector blocked thermal emission from the hot test gases. An identical bandpass filter was placed before the reference detector in order to balance its spectral modulation on the reference beam. Irises in both beam paths controlled the power incident on each detector.

The QCL was driven with a pulsed current source (Lightwave LDP-3830) at an injection current of 1.45 A with a 2 μs pulse period and 100 ns pulse width (5% duty cycle). The germanium AOM was driven by an RF generator at frequencies around 40 MHz. The RF generator output frequency was modulated as a saw-tooth wave by a function generator, which was synchronized with the laser driver pulses. The frequency sweep of 65 μs duration swept the entire ~200 cm^{-1} QCL bandwidth, which optimized the tradeoff between spectral sampling (points per spectrum) and temporal resolution (spectra per second). There were 30 laser pulses during each sweep, giving an effective spectral resolution of 6.7 cm^{-1} between each point. Due to the 8–20 cm^{-1} spectral width of the laser emission (Fig. 2), the achieved spectral resolution was 10–15 cm^{-1} on average.

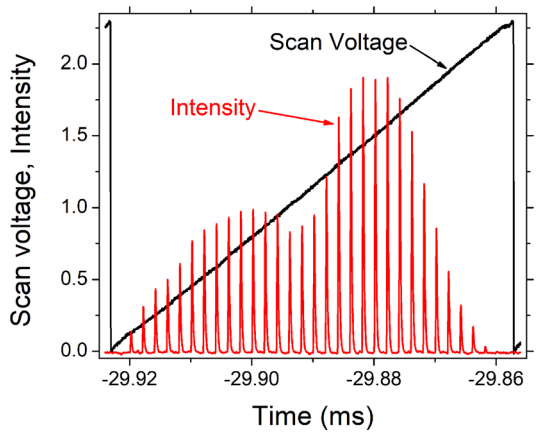

Fig. 4 Example traces of RF generator control voltage, corresponding to AOM driving frequency, and pulsed QCL output intensity for the transmitted signal of the shock tube experiment before the arrival of the incident shock wave

The pressure at the test location, beam intensities, and AOM control voltage were all recorded on a digital oscilloscope (Tektronix MDO3104) with 50 MHz sampling rate for a duration of 100 ms. An example of the transmitted laser intensity and RF generator control voltage (corresponding to AOM driving frequency) during a single spectral sweep is presented in Fig. 4. The 30 laser pulses and their envelope of peak power are evident. The time axis is linearly proportional to the frequency axis due to the linear sweep of AOM driving frequency. Negative values of time correspond to times before the arrival of the shock wave into the path of the beam. This intensity envelope differs somewhat from that in Fig. 2, where the AOM control voltage was fixed for each spectrum, due to the swept mode of operation and spectral modulation due to elements such as filters and mirrors in the beam path. The FTIR data of Fig. 2 were nevertheless used to define the starting and stopping wavenumber of each sweep.

With a spectral sweep period of 65 μs, a total of approximately 1500 spectra were recorded over the course of a single shock experiment. Each spectrum of the transmitted beam is attenuated by species having absorption features in the spectral range of the system and by analyzing the profiles of each spectrum, the concentrations of those species may be determined.

Mixture Preparation. The test mixture was prepared manometrically in a 33 L Teflon-coated high-purity stainless steel mixing facility. Partial pressures were measured using a 10,000 Torr full scale range Baratron (MKS Baratron 628ED, 0.25% readout accuracy). Research grade (purity >99.999%) argon and atomic absorption grade (>99.5%) N_2O were used to prepare the test mixture of 10% N_2O in balance argon. The mixture was allowed to mix for at least eight hours before any experiments were performed. At high pressures and temperatures such as those achieved in this study, N_2O breaks down to form NO, which was the target species to be measured.

According to chemical kinetic simulations performed using CHEMKIN PRO [23] and the Lawrence Livermore National Laboratory (LLNL) NO_x chemical kinetic mechanism [24]. Nitrous oxide shock heated to a temperature of 2100 K at a pressure of 5 atm decomposes into NO within approximately 100 μs, after which point the concentration of NO remains constant. A mixture of N_2O in a bath gas of argon was thus selected to evaluate the AOM QCL system's capabilities of retrieving NO concentration.

Data Analysis. Transmittance spectra were analyzed according to the Beer–Lambert law

$$\alpha(\nu) = -\ln\left(\frac{I(\nu)}{I_0(\nu)}\right) = \sigma(\nu)\frac{P}{R_u T}xL \tag{1}$$

where $\alpha(\nu)$ is the absorption coefficient, $I(\nu)$ and $I_0(\nu)$ are the transmitted and reference beam intensities, $\sigma(\nu)$ (cm^2/mol) is the absorption cross section at frequency ν, P is the total pressure (atm), R_u is the universal gas constant (cm^3 atm/mol K), x is the mole fraction of the absorbing species, and L is the optical path length (cm).

Spectra were recorded sequentially on an oscilloscope, whose time scale is converted to wavenumbers using the recorded AOM control voltage trace (Fig. 4) and the FTIR spectral calibration (Fig. 2). For the purpose of obtaining a concentration time history, each spectrum is time stamped according to the center of the AOM control-voltage sweep. Because the beam transmitted through the shock tube passes through two ZnSe windows that are absent from the path of the reference beam, there is a slight difference in their recorded power spectra, resulting in artifacts in the calculated transmittance according to Eq. (1). The effects of the differences in the beam paths are accounted for by a baseline correction which consisted of normalizing each reference spectrum to an averaged transmitted spectrum, which was recorded through the evacuated shock tube prior to the experiment. A new vacuum reference spectrum was taken prior to each experiment in order to account for any long-term drift in the system output. For both the reference and transmitted beams, the maximum intensity of each individual 100 ns QCL pulse is recorded and assigned to its corresponding peak wavenumber, giving $I_0(\nu)$ and $I(\nu)$ data for absorbance calculation by Eq. (1).

The NO mole fraction is found from the spectrally integrated absorbance and absorption cross section $\sigma(\nu)$ according to

$$x_{NO} = \frac{R_u T_5 \int \alpha(\nu) d\nu}{P_5 L \int \sigma(\nu) d\nu} \tag{2}$$

where the integration range was 1750–1900 cm^{-1}. For the purposes of calculating NO mole fraction, the pressure P_5 and temperature T_5 were assumed to be constant over the duration of the experiment. The absorption cross section of NO was first obtained from HITRAN [25] at the experimental conditions and then convolved with a 15 cm^{-1} FWHM Gaussian function to account for the linewidth of each of the laser output lines. The NO concentration was determined from all spectra to reveal its temporal dynamics during the shock reaction. The NO time evolution was compared to predictions of chemical kinetic simulations (CHEMKIN PRO [23]) using the Lawrence Livermore National Laboratory (LLNL) NO_x chemical kinetic mechanism [24].

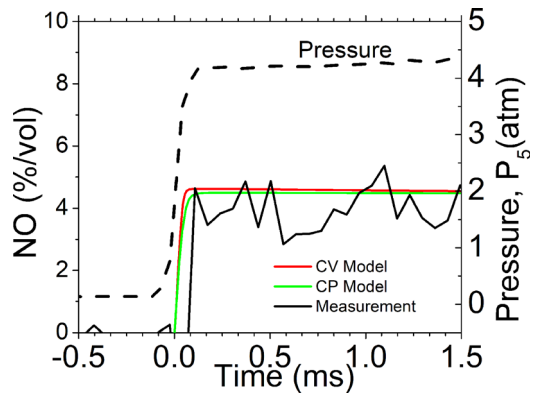

Fig. 5 Pressure and NO mole fraction transients for $T_5 = 2080$ K, $P_5 = 4.2$ atm shock experiment

Results and Discussion

Shock tube experiments were performed with temperatures ranging from $T_5 = 1245$–2517 K and pressures ranging from $P_5 = 3.6$–5.8 atm. The pressure trace for a shock experiment with test conditions $T_5 = 2080$ K and $P_5 = 4.2$ atm experiment is shown in Fig. 5.

Chemical kinetic simulations predict that the NO concentration is independent of minor pressure fluctuations in reflected shock region, such as those of the magnitude observed in this experiment, justifying the assumption of constant pressure used in the modeling (to represent the thermodynamic conditions inside the shock tube) and analysis.

The difference spectra of the measured transmitted and reference beam intensities for times before the arrival of the incident shock and after the reflected shock are shown in Fig. 6. Before the shock, there is no absorption of the transmitted signal by the initial N_2O/Ar mixture. The difference spectrum seen in Fig. 6(*a*) is nonzero due to the differences in optical components seen by the reference and transmitted signals but is constant across scans. This constant difference spectrum is accounted for by baseline correction in the data analysis procedure when calculating concentrations. After the reflected shock, the difference spectrum shows a clear change in shape, particularly on the right-hand side (higher frequency band) of each spectral scan, as seen in Fig. 6(*b*). The transmitted beam is attenuated due to absorption by the reaction product NO, resulting in a decrease in the difference spectrum.

The NO concentration and pressure transients are presented in Fig. 5. Pressure values are temporal averages over the duration of each spectral sweep, resulting in the characteristic distinct spikes due to the incident and reflected shock waves becoming averaged. Measured and modeled NO mole fractions are in good agreement. Measurement noise is attributed to beam deflection caused by fast turbulence and shot-to-shot variance in the laser output intensity. The estimated uncertainty in the measured mole fraction due to these effects and due to uncertainty in the spectral overlap between the fine mode structure of the laser output and absorption features of NO is approximately ±20%, given by the standard deviation of the measured NO mole fraction.

Figure 7 presents the absorbance spectrum averaged over ~200 spectral sweeps recorded after the arrival of the reflected shock wave. This is compared to a spectrum calculated from HITRAN cross-sectional data after convolution with a 15 cm^{-1} wide Gaussian function that simulates the system spectral resolution. In the high wavenumber region above ~1850 cm^{-1}, there is good agreement between the theoretical absorption spectrum and measured

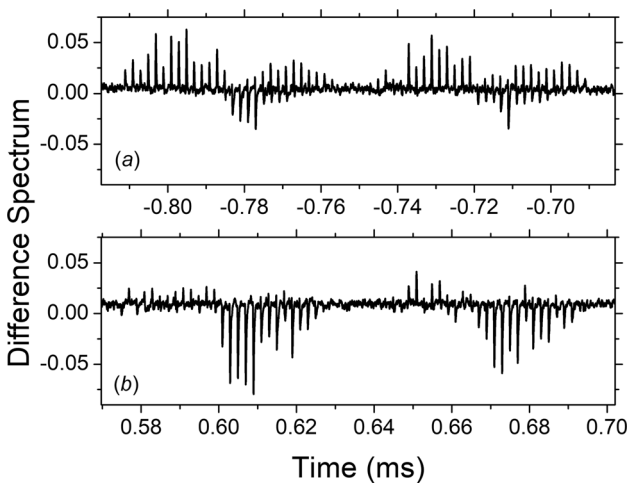

Fig. 6 Sample consecutive difference spectra of the transmitted and reference beams before arrival of the shock (*a*) and after the reflected shock wave (*b*). There is a clear change due to absorption from the NO formed.

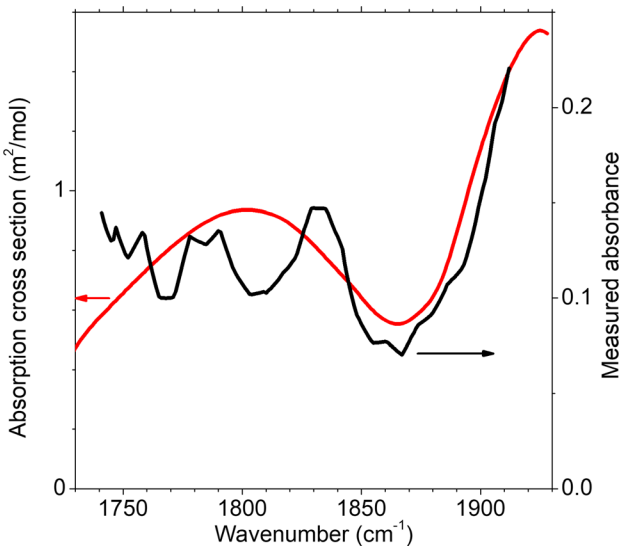

Fig. 7 Theoretical NO absorption spectrum at $T = 2080$ K, $P = 4.2$ atm, as observed with a 15 cm^{-1} linewidth Gaussian instrument function spectrometer (red) and averaged observed absorbance spectra over course of test time (black)

absorbance spectrum. The differences below 1850 cm^{-1} may be due to the presence of other absorbing species or to mismatch between interleaved laser mode structure and molecular absorption fine structure.

Plots of the theoretical NO absorption cross section (convoluted with a 15 cm^{-1} linewidth Gaussian function) and normalized measured absorbance spectra for different temperatures ranging from 1245–2517 K are shown in Fig. 8.

As shown in Figs. 8(*a*)–8(*c*), as temperature increases the relative height between the two peaks of NO absorption in this portion of the spectrum decreases, and the center of the left peak (around 1815 cm^{-1} at 1245 K) moves toward lower wavenumbers. The measured absorbance spectra of Figs. 8(*d*)–8(*f*) clearly capture this change in the NO absorption spectrum with temperature. The valley between the two peaks is most pronounced in Fig. 8(*d*) for the $T = 1245$ K experiment, and the valley becomes shallower as the temperature is increased, as shown in Figs. 8(*e*) and 8(*f*).

Our experiments demonstrate the AOM QCL system's ability to distinguish temperature changes via evolution of the measured spectral profile and for quantifying the temporal evolution of NO concentrations at time-scales relevant to turbulent combustion reactions at high pressures and temperatures similar to those that may be found in the combustors of gas turbines.

In the configuration used in this study, the temporal and spectral resolution of the system were limited due to hardware constraints, but these may be improved to yield better system performance as follows. The temporal resolution of the measurement scheme can be improved by using a laser driver that can exceed 5% duty cycle. The duration of the applied current pulse must be at least 100 ns for the laser output to stabilize, so the 5% duty limit of our driver limits the pulse repetition rate to 500 kHz, which is, in turn, the maximum spectral sampling rate. With a fixed laser pulse rate, there is a tradeoff between scan speed and spectral density of sampled points. The spectral separation of the acquired data does not need to be smaller than about half the laser linewidth or ~7 cm^{-1}. Thus, to span the ~200 cm^{-1} gain band width of the QCL, we need to sample ~28 points. A 500 kHz repetition rate gives a minimum useful spectral scan duration of 56 μs. Temporal resolution is most simply increased by using a pulsed current source with a higher duty cycle. For example, using a duty cycle of 50% would allow for a 5 MHz pulse repetition rate and a full spectral sweep in as little as 5.6 μs. This would improve the temporal resolution of the measurement system to better than necessary to follow any anticipated fluctuations in chemical composition in a combustion reaction. Shot-to-shot variations in the laser output intensity may also be partially attributed to instability in the pulsed laser driver, so the use of a more stable driver would result in an improved signal to noise ratio and reduced uncertainty in the measured spectral profile and corresponding mole fractions.

The spectral resolution of the measurement is ultimately limited by the minimum laser linewidth at each AOM output setting. The minimum laser line width for a given beam size depends on the AOM and duration of the QCL pulse. By adjusting the AOM optical configuration and QCL driving current parameters, the linewidth may be reduced, allowing improved spectral resolution. Linewidths can be as narrow as 2.5 cm^{-1} in pulsed operation, and 1.2 cm^{-1} in CW operation [19]. The actual absorption spectrum of NO, even at high temperatures and pressures, is not smooth as suggested in Fig. 7 after convolving with a 15 cm^{-1} instrument function. In reality, only select modes of the laser output spectrum

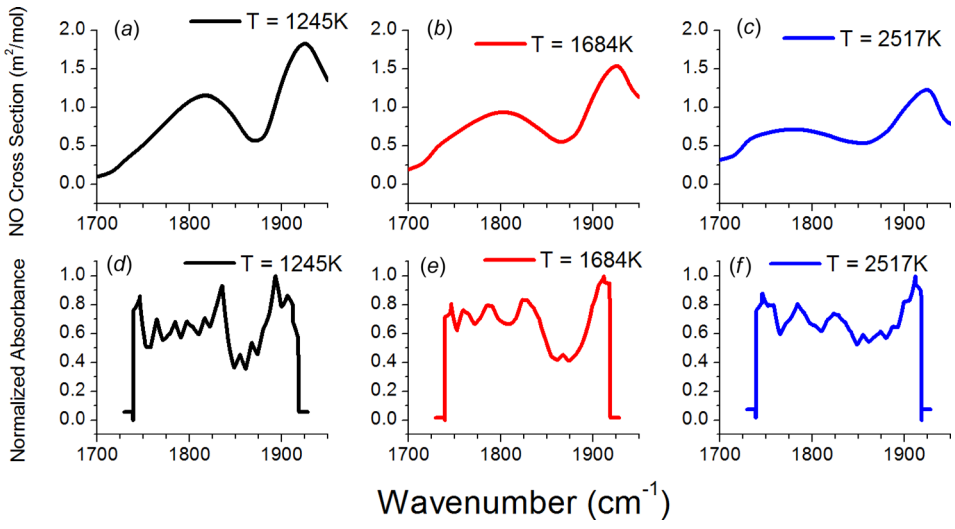

Fig. 8 ((*a*)–(*c*)): Absorption cross section of NO convoluted with a 15 cm^{-1} Gaussian instrument function at (*a*) $T = 1245$ K, (*b*) $T = 1684$ K, and (*c*) $T = 2517$ K obtained from HITRAN [25]. ((*d*)–(*f*)): Average measured absorbance spectra (normalized to peak value) over the course of the test time for experiments with corresponding temperatures.

structure (as seen in Fig. 2) may coincide with absorption peaks. This effect is not accounted for in the analysis procedure applied in this study. To correctly model the absorption of the system, the output spectrum of each of the laser lines must be characterized and used along with a high-resolution absorption spectrum of the species of interest to calculate the absorbance experienced at each laser output setting. The different absorption efficiencies for each line may partially explain why the observed NO mole fraction is less than predicted by the chemical kinetics model, as well as why there is so much artificial structure in the measured absorbance below 1850 cm^{-1} (Fig. 7). By reducing the output linewidth and further characterizing the spectral profile of the system over the range of operating conditions, the spectral resolution may be improved, leading to increased temperature sensitivity and improving the system's ability to measure multiple species simultaneously.

Moving forward, the temporal and spectral resolution of the AOM QCL diagnostic scheme will be improved as discussed. Further experiments will be performed to characterize the ability of the system to simultaneously measure multiple species (e.g., NO and formaldehyde, both of which have absorption features in this range of the MIR) and temperature. The system performance will then be validated in experiments with fuels and conditions representative of those common in gas turbine combustor settings. Also, additional lasers at other wavelengths in the MIR region will be developed and used to probe other combustion species of interest (e.g., CO near 4.6 μm, CO_2 near 4.2 μm, etc.). Ultimately, field demonstration of the system with gas turbine combustors will be conducted in collaboration with industry partners.

Conclusion

This work provides the first demonstration of an acousto-optically modulated external cavity configuration quantum cascade laser system applied to combustion diagnostics. The system was used to obtain time-resolved spectral measurements of NO formation behind reflected shock waves at temperatures of 1245–2517 K and pressures of 3.6–5.8 atm. Concentration time-history measurements agreed with chemical kinetic simulations. The time-averaged absorption spectra were in good agreement with the NO absorption spectrum predicted by HITRAN over a range of temperatures, demonstrating the potential of the system to provide simultaneous concentration and temperature measurements. Furthermore, the broad (~200 cm^{-1}) spectral range of the system has potential to be applied to simultaneously monitor multiple absorbing species with a single line of sight measurement. Spectral resolution was limited by laser driver duty cycle, and laser emission bandwidth. Improvements to the AR coating and use of a laser driver with higher duty cycle would enable temporal resolution better than 10 μs or spectral resolution better than a few wavenumbers. The work presented here is a first step toward fast, simultaneous, multispecies measurements in the midinfrared region using a single QCL during combustion and has tremendous potential for combustion science. The simplicity of the setup compared to using multiple lasers makes it promising for practical combustion sensing in applications such as gas turbine combustors.

Acknowledgment

Any opinions, findings, and conclusions or recommendations expressed in this material are those of the author and do not necessarily reflect the views of the National Science Foundation. A.L and P.F. acknowledge start-up support from the Nanoscience Technology Center and the University of Central Florida. The authors thank assistance from Owen Pryor and Joseph Lopez during UCF shock tube experiments. Acknowledgement is given to Dr. Bill Partridge Jr. (Oak Ridge National Lab) and Professor Konstantin Vodopyanov (UCF) for suggestions regarding the experimental set up. AVM, PNF, and REP are members of, and have financial interest in, Truventic LLC.

Funding Data

- Air Force Research Laboratory under STTR Phase I Contract No. FA8650-16- P-2706 to Truventic and UCF.
- National Science Foundation Graduate Research Fellowship Program (Grant No. 1144246).

References

[1] Manikantachari, K. R. V., Vesely, L., Martin, S., Bobren-Diaz, J. O., and Vasu, S., 2018, "Reduced Chemical Kinetic Mechanisms for Oxy/Methane Supercritical CO2 Combustor Simulations," ASME J. Energy Resour. Technol., **140**(9), p. 092202.
[2] Khadse, A., Blanchette, L., Kapat, J., Vasu, S., Hossain, J., and Donazzolo, A., 2018, "Optimization of Supercritical CO2 Brayton Cycle for Simple Cycle Gas Turbines Exhaust Heat Recovery Using Genetic Algorithm," ASME J. Energy Resour. Technol., **140**(7), p. 071601.
[3] Pryor, O., Barak, S., Lopez, J., Ninnemann, E., Koroglu, B., Nash, L., and Vasu, S., 2017, "High Pressure Shock Tube Ignition Delay Time Measurements During Oxy-Methane Combustion With High Levels of CO_2 Dilution," ASME J. Energy Resour. Technol., **139**(4), p. 042208.
[4] Gupta, A. K., and Breault, R. W., 2018, "Special Issue: Selected Papers From the 42th International Technical Conference on Clean Coal and Fuel Systems," ASME J. Energy Resour. Technol., **140**(6), p. 060301.
[5] Dumitrescu, C. E., Cheng, A. S., Kurtz, E., and Mueller, C. J., 2017, "A Comparison of Methyl Decanoate and Tripropylene Glycol Monomethyl Ether for Soot-Free Combustion in an Optical Direct-Injection Diesel Engine," ASME J. Energy Resour. Technol., **139**(4), p. 042210.
[6] Nash, L., Klettlinger, J., and Vasu, S., 2017, "Ellipsometric Measurements of the Thermal Stability of Alternative Fuels," ASME J. Energy Resour. Technol., **139**(6), p. 062207.
[7] Bezergianni, S., Dimitriadis, A., Kikhtyanin, O., and Kubička, D., 2018, "Refinery Co-Processing of Renewable Feeds," Prog. Energy Combust. Sci., **68**, pp. 29–64.
[8] Knothe, G., and Razon, L. F., 2017, "Biodiesel Fuels," Prog. Energy Combust. Sci., **58**, pp. 36–59.
[9] Nabagło, D., Kurek, T., and Wojdan, K., 2018, "Combustion Process Analysis and Diagnostic Using Optical Flame Scanners in Front-Fired Pulverized Coal Boiler," ASME J. Energy Resour. Technol., **140**(7), p. 072003.
[10] Glarborg, P., Miller, J. A., Ruscic, B., and Klippenstein, S. J., 2018, "Modeling Nitrogen Chemistry in Combustion," Prog. Energy Combust. Sci., **67**, pp. 31–68.
[11] Kohse-Höinghaus, K., 2018, "Clean Combustion: Chemistry and Diagnostics for a Systems Approach in Transportation and Energy Conversion," Prog. Energy Combust. Sci., **65**, pp. 1–5.
[12] Koroglu, B., Pryor, O., Lopez, J., Nash, L., and Vasu, S. S., 2016, "Shock Tube Ignition Delay Times and Methane Time-Histories Measurements During Excess CO2 Diluted Oxy-Methane Combustion," Combust. Flame, **164**, pp. 152–163.
[13] Pryor, O. M., Barak, S., Koroglu, B., Ninnemann, E., and Vasu, S. S., 2017, "Measurements and Interpretation of Shock Tube Ignition Delay Times in Highly CO2 Diluted Mixtures Using Multiple Diagnostics," Combust. Flame, **180**, pp. 63–76.
[14] Barari, G., Pryor, O., Koroglu, B., Lopez, J., Nash, L., Sarathy, S. M., and Vasu, S. S., 2017, "High Temperature Shock Tube Experiments and Kinetic Modeling Study of Diisopropyl Ketone Ignition and Pyrolysis," Combust. Flame, **177**, pp. 207–218.
[15] Koroglu, B., and Vasu, S. S., 2016, "Measurements of Propanal Ignition Delay Times and Species Time Histories Using Shock Tube and Laser Absorption," Int. J. Chem. Kinet., **48**(11), pp. 679–690.
[16] Almodovar, C. A., Spearrin, R. M., and Hanson, R. K., 2017, "Two-Color Laser Absorption Near 5 μm for Temperature and Nitric Oxide Sensing in High-Temperature Gases," J. Quant. Spectrosc. Radiat. Transfer, **203**, pp. 572–581.
[17] Lyakh, A., Barron-Jimenez, R., Dunayevskiy, I., Go, R., and Patel, C. K. N., 2015, "External Cavity Quantum Cascade Lasers With Ultra Rapid Acousto-Optic Tuning," Appl. Phys. Lett., **106**(14), p. 141101.
[18] Lyakh, A., Barron-Jimenez, R., Dunayevskiy, I., Go, R., Tsvid, G., and Patel, C. K. N., 2016, "Continuous Wave Operation of Quantum Cascade Lasers With Frequency-Shifted Feedback," AIP Adv., **6**(1), p. 015312.
[19] Lyakh, A., Barron-Jimenez, R., Dunayevskiy, I., Go, R., Tsvid, E., and Patel, C. K. N., 2016, "Progress in Rapidly-Tunable External Cavity Quantum Cascade Lasers With a Frequency-Shifted Feedback," Photonics, **3**(2), p. 19.
[20] Loparo, Z. E., Lopez, J. G., Neupane, S., Partridge, W. P., Vodopyanov, K., and Vasu, S. S., 2017, "Fuel-Rich n-Heptane Oxidation: A Shock Tube and Laser Absorption Study," Combust. Flame, **185**(Suppl. C), pp. 220–233.
[21] Ninnemann, E., Koroglu, B., Pryor, O., Barak, S., Nash, L., Loparo, Z., Sosa, J., Ahmed, K., and Vasu, S., 2018, "New Insights Into the Shock Tube Ignition of

H2/O2 at Low to Moderate Temperatures Using High-Speed End-Wall Imaging," Combust. Flame, **187**(Suppl. C), pp. 11–21.
[22] Barak, S., Pryor, O., Lopez, J., Ninnemann, E., Vasu, S., and Koroglu, B., 2017, "High-Speed Imaging and Measurements of Ignition Delay Times in Oxy-Syngas Mixtures With High CO_2 Dilution in a Shock Tube," ASME J. Eng. Gas Turbines Power, **139**(12), p. 121503.
[23] ANSYS, 2017, "ANSYS Chemkin-Pro," ANSYS, Inc., San Diego, CA accessed Jan. 1, 2017, http://www.ansys. com/products/fluids/ansys-chemkin-pro
[24] Hori, M., Matsunaga, N., Marinov, N., William, P., and Charles, W., "An Experimental and Kinetic Calculation of the Promotion Effect of Hydrocarbons on the NO-NO2 Conversion in a Flow Reactor," Proc. Symp. (Int.) Combust., **27**(1), pp. 389–396.
[25] Rothman, L. S., Gordon, I. E., Babikov, Y., Barbe, A., Benner, D. C., Bernath, P. F., Birk, M., Bizzocchi, L., Boudon, V., and Brown, L. R., 2013, "The HITRAN2012 Molecular Spectroscopic Database," J. Quant. Spectrosc. Radiat. Transfer, **130**, pp. 4–50.